Variability in the Wave Climate of the North Pacific: Links to Inter-Annual and Inter-Decadal Variability

Nicholas E. Graham
Scripps Institution of Oceanography and
Hydrologic Research Center

Variability in the wave climate of the North Pacific is of interest from many perspectives including coastal management, near-shore engineering, sediment transport and beach erosion, and maritime safety. Recent results [1,2] document variability in North Pacific winter wave heights (both averages and extremes) over the past 40-50 years as seen in hindcasts produced with wave models driven with winds from the National Centers for Environmental Prediction (NCEP) reanalysis. This variability is marked by changes at a variety of time scales ranging from inter-annual to multi-decadal, the latter dominated by an upward trend in wave heights over much of the eastern North Pacific. It is of interest to link these changes to the dominant modes of circulation variability over the North Pacific, most notably the El Niño-Southern Oscillation (ENSO) and Pacific inter-decadal variability (often referred to as the Pacific Decadal Oscillation or PDO). Numerous useful references discuss these modes of variability and their expression over the North Pacific (e.g., [3,4]) and the interested reader is directed to those papers, and references therein, for more detailed descriptions. For this discussion, suffice it to note that during El Niño episodes, and during periods when the PDO index is high, North Pacific winter cyclones tend to be stronger and tend to track farther to the south and east. Such changes in cyclone behavior have important effects on wave climate. This note examines how ENSO and PDO variability are reflected in hindcast North Pacific winter wave climate [as seen in a 50-year hindcast with the WAVEWATCH III model [5,1]. To give an example how changes in the large-scale wave climate are expressed in regional coastal waters, results are also shown from a derivative data set created by transforming 3-hourly hindcast deep-water wave spectra from a point just off Point Conception into the Southern California Bight (the transformation functions were produced using the model of [6]). Other results, most relevant to multi-decadal changes, come from a statistically derived hindcast for the winter North Pacific from 1899-2000 using techniques similar to those applied by [7] in their study of wave trends in the North Atlantic.

Fig. 1 [1] shows linear trends in hindcast 95th percentile significant wave height (H_S) for December-March 1948/49 though 1997/98. These trends reach values above 2 meters in the central North Pacific and reach 30-35% of the 50-year winter mean in the region south of 35°N and east of 150°W. To get an idea of how these large-scale trends have affected the coast of southern California, Fig. 2 (lower panel) shows linear trends in 99th percentile H_S after transformation into the Southern California Bight. One feature of note is that the largest trends are found in to the south and east of the

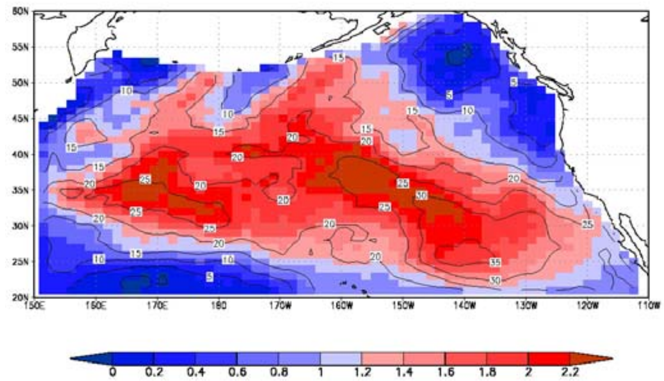

Fig. 1. Trends in 99th percentile December-March wave heights from the WAVEWATCH III hindcast for 1948/49 – 1997/98. Colors indicate linear trends (per 50 years) in meters. Contours show trend as a percentage of the mean 99th percentile wave height.

offshore islands and shoals. This pattern results both from the general upward trend in wave heights and an associated tendency towards more westerly approach directions as the storm track moved south. This latter effect acts to reduce sheltering to the south and east of the islands and shoals thus producing enhanced trends in those regions. Fig. 3 (upper panel) shows the trends (repeated in Fig. 3, lower panel) expressed as fractions of the long-term mean 99th percentile H_S (Fig. 2, upper panel). Note that the regions with the largest relative trends correspond well with the regions where the average extreme wave heights are lowest. This correspondence reflects the trend towards more westerly approach directions.

Focusing now specifically on El Niño variability, Fig. 4 shows correlations between 95th percentile December-March H_S and sea surface temperature anomalies (SSTA) in the NINO3 region (a commonly used index of El Niño activity; area-averaged SSTS for 150°W to 90°W and 5°N-5°S). These correlations reach up to 0.6 (about the same magnitude as for many indices of atmospheric circulation) in the southeast part of the domain. This distribution reflects both the tendency for stronger storms that track farther south and east during El Niño winters and swell propagation into the sub-tropical Northeast Pacfic. Over the Southern California Bight the correlations with NINO3 SSTA (Fig. 5) show a relatively complicated pattern (in comparison with Figs. 2 and 3) with a general tendency for lower correlations in inshore waters. Fig. 5 also shows the portion of the variability in 95th percentile H_S explained (through linear regression) by ENSO variability expressed as a fraction of the mean 95th percentile H_S. The pattern is similar to that for the relative

0-933957-31-9

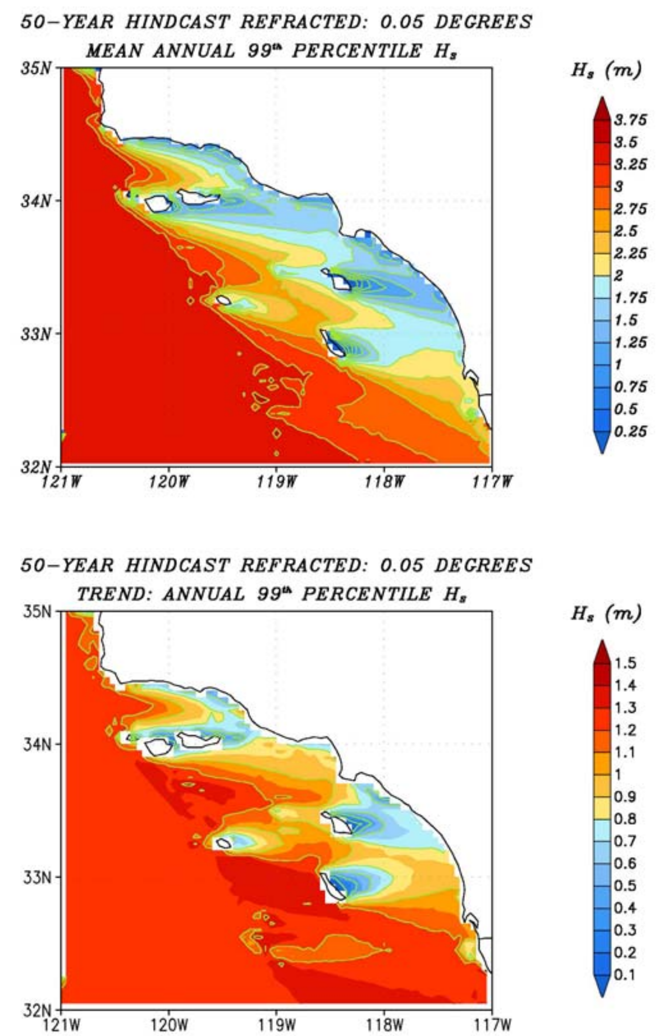

Fig. 2. Linear trend in 99th percentile significant wave (lower). Long-term mean 99th percentile significant wave height (upper).

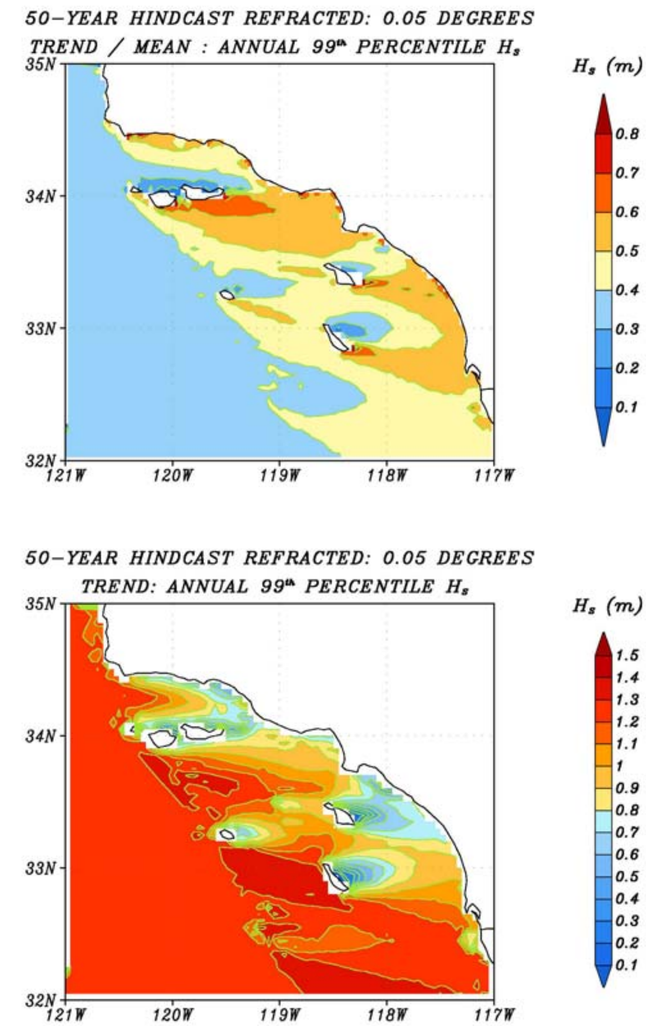

Fig. 3. As in Fig. 2 but lower panel shows linear trend in 99th percentile significant wave expressed as a percentage of the long-term mean 99th percentile significant wave height.

trend (Fig. 3), with the largest relative ENSO-associated changes tending to occur where mean extreme heights are low.

Turning now to the PDO and very long time scales, a statistical wave hindcast was developed for December-March 90th percentile H_S for 1899-2000. This was done by relating average December-March sea level pressure (SLP) to hindcast 90th percentile wave statistics. The methodology applied was similar to that used by [7] and [2] and uses the first few principle components of the hindcast wave and SLP fields as the basis for a field-to-field linear regression model. The essential idea is to derive a robust low-order function whose input is mean December-January sea level pressure and whose output is 90th percentile wave heights. This function was derived using the hindcast wave fields and historical SLP data for 1947-48 to 1997-98 and then applied to SLP data for the entire century.

Fig. 6 compares 90th percentile wave heights derived from the numerical wave model and using the statistical approach for a location off Point Conception. The agreement between the two estimates is good (the correlation is 0.84), particularly so if the results are smoothed. These results suggest that the period of large extreme wave heights in the 1980's and 1990's was not matched during the century, though the late 1930's and early 1940's also showed a period of relatively high values. Fig. 7 compares the statistically derived record of extreme wave heights for Point Conception with the December-March PDO index (see [4] – the index is a measure of large-scale SST changes across the North Pacific). Although the agreement in year-to-year changes is not particularly good (the correlation is 0.53), after smoothing with an 11-year running mean both series show similar patterns of low frequency variability. This result, consistent those of [2], suggests that the trends in North Pacific wave heights seen in the 50-year hindcast are related to inter-decadal trends over the North Pacific and the particular period covered by the NCEP reanalysis results in especially large trends. Nevertheless, the latter two decades of the 20th century stand out as in terms of extreme wave heights in the eastern North Pacific.

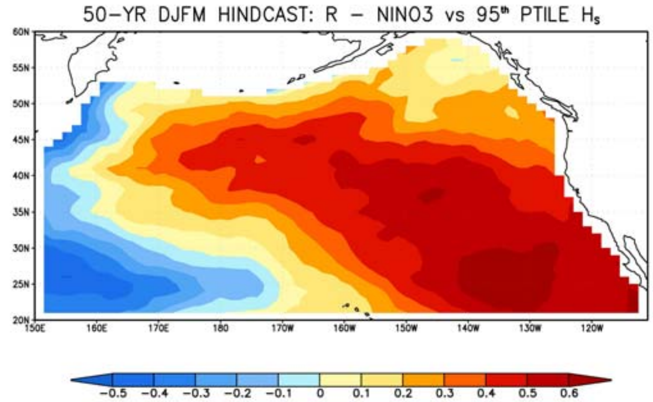

Fig. 4. Correlations between hindcast December-March wave height and NINO3 SST; 1948/49 to 1997/98.

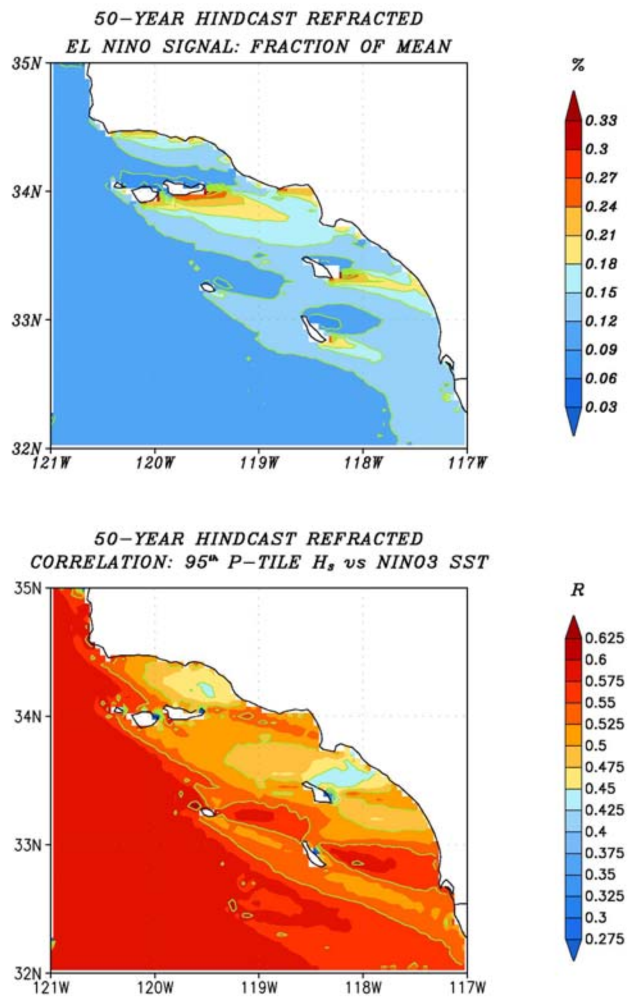

Fig. 5. Correlations between 95th percentile significant wave height and NINO3 SST (lower; Dec.-March 1948/49 – 1997/98) and magnitude of variability associated with El Niño as a fraction of mean 95th percentile wave height

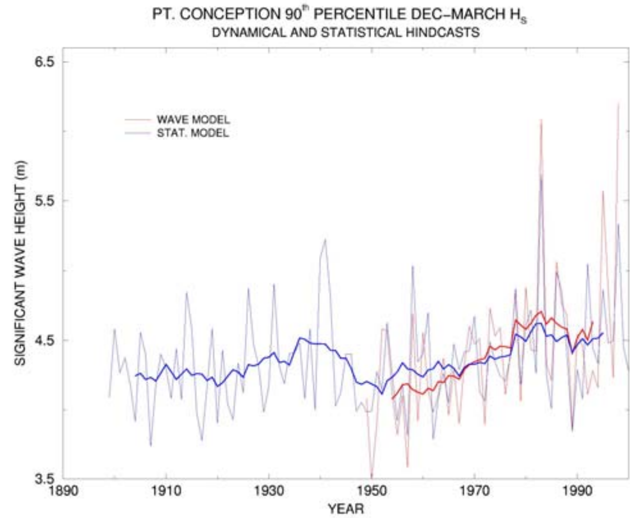

Fig. 6. Annual 90th percentile wave heights for a locations near Point Conception: WAVEWATCH III model hindcast (thin red line) and SLP-based statistical hindcast (thin blue line); thick lines show 7-year running averages.

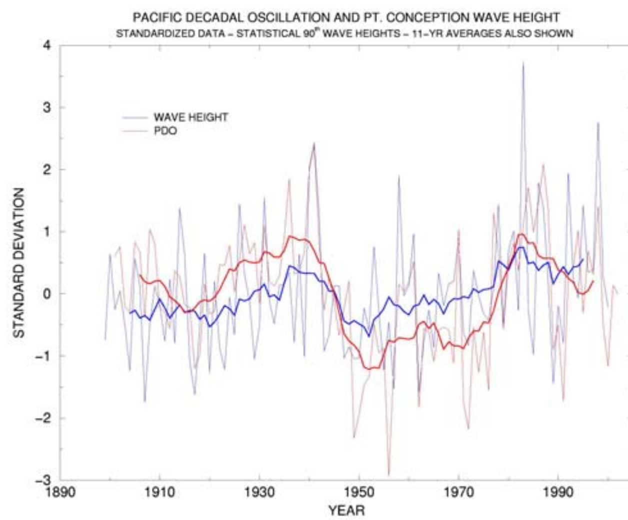

Fig. 7. Annual 90th percentile wave heights for a locations near Point Conception from the SLP-based statistical hindcast (thin blue line) and December-March Pacific Decadal Oscillation time series (thin red line); thick lines show 7-year running averages.

References

[1] Graham, N. E. and H. Diaz, 2001: Evidence for intensification of North Pacific winter cyclones since 1948, Bull. Amer. Met. Soc., 82, 1869-1893.

[2] Wang, X. L., and V. R. Swail, 2001: Changes in extreme wave heights in the Northern Hemisphere Oceans and related atmospheric circulation regimes, J. Climate, 14, 2204-2221

[3] Trenberth, K. E., and J. W. Hurrell, 1994: Decadal atmosphere-ocean variations in the Pacific, Clim. Dyn., 9, 303-319.

[4] Mantua, N. J., S. R. Hare, Y. Zhang, J. M. Wallace and R. C. Francis, 1997: A Pacific interdecadal oscillation with impacts on salmon production, Bull. Amer. Met. Soc., 78,1069-1079.

[5] Tolman, H. L., 1999; User manual and system documentation of WAVEWATCH III, version 1.18, U. S. Dept. of Commerce, NOAA, NWS, NCEP, Ocean Modeling Branch Contribution 166, 4700 Silver Hill Road, Mail Stop 9910, Washington, D. C. 20233-9910, 112pp.

[6] O'Reilly, W., 1991: Modeling surface gravity waves in the Southern California Bight, Ph. D. dissertation, Scripps Institution of Oceanography, La Jolla, CA, 92093, 90 pp.

[7] Kushnir, Y., V. J. Cordone, and J. G. Greenwood, 1997: The recent increase in North Atlantic wave heights, J. Climate, 10, 2107-2113.

.